Frontiers in Bioscience Landmark

Front. Biosci. (Landmark Ed) **2023**; 28(8): 164
https://doi.org/10.31083/j.fbl2808164

Original Research

Exploring the Underlying Mechanism of *Alpinia officinarum* Hance Ameliorating Diabetic Gastroparesis through Combining Network Pharmacology, Molecular Docking, and *in Vivo* Experimental Verification

Xiuwen Zheng[1,2,†], Yuxin Zhang[1,2,†], Jian Xu[1], Xiangyi Li[1,2], Huan Wen[1,2], Xuguang Zhang[1,2], Aixia Liu[1,2], Junqing Zhang[1,2,*]

[1]Hepatobiliary and Liver Transplantation Department of Hainan Digestive Disease Center, The Second Affiliated Hospital of Hainan Medical University, 571199 Haikou, Hainan, China
[2]Hainan Provincial Key Laboratory for Research and Development of Tropical Herbs, Haikou Key Laboratory of Li Nationality Medicine, School of Pharmacy, Hainan Medical University, 571199 Haikou, Hainan, China
*Correspondence: hy0207002@hainmc.edu.cn (Junqing Zhang)
[†]These authors contributed equally.
Academic Editor: Jen-Tsung Chen
Submitted: 11 January 2023 Revised: 26 February 2023 Accepted: 6 March 2023 Published: 11 August 2023

Abstract

Background: *Alpinia officinarum* Hance (AOH) has a long history in China as a Chinese medicine and exerts the pharmacological effects of antidiabetic and gastrointestinal protection. In traditional Chinese medicine theory, AOH is often combined with other Chinese medicines for the treatment of diabetic gastroparesis (DGP). However, the molecular mechanisms, potential targets, and bioactive ingredients of AOH that act against DGP are yet to be elucidated. In this study, network pharmacology, molecular docking, and experimental study were used to predict the therapeutic effects and the potential molecular mechanism of AOH in DGP. **Methods**: Network pharmacology analysis was performed to acquire information on the active chemical ingredients, DGP-related target proteins in AOH, and potential signaling pathway. In addition, molecular docking approach was used to simulate the binding of drugs and targets. Finally, DGP-mice model was used for experimental verification *in vivo*. **Results**: Through the network pharmacological research, AKT1 was found to be the core protein in AOH for the treatment of DGP and was mainly involved in the PI3K-AKT signaling pathway. Additionally, the interactions between bioactive compounds and target proteins (PIK3CA and AKT1) were analyzed using molecular docking, which verified the results of network pharmacology. Further *in vivo* studies indicated that AOH could reduce fasting blood glucose levels, improve gastric emptying rate, and ameliorate biochemical indicators in DGP mice. Moreover, AOH could increase the expressions and phosphorylation levels of PI3K and AKT in the stomach to regulate oxidative stress. **Conclusions**: The study has shown that AOH may play a protective role on DGP through mediation of the PI3K-AKT signaling pathway to regulate oxidative stress.

Keywords: *Alpinia officinarum* Hance; diabetic gastroparesis; network pharmacology; molecular docking; experimental verification

1. Introduction

Diabetic gastroparesis (DGP) is a common diabetes-related complication, which is defined as abnormally delayed gastric emptying of solid food in the absence of mechanical obstruction [1–3]. The disease is caused by certain abnormal physiological conditions, such as abnormal gastric smooth muscle motility, delayed gastric emptying, and dysrhythmia of the gastric electrical rhythm, and the major symptoms are early satiety, abdominal distension, vomiting, and epigastric pain [4,5]. Although the pathogenesis of DGP is elusive, it has been reported to be associated with dysglycemia, oxidative stress, gastrointestinal neuropathy, gastric smooth muscle lesions, and interstitial cells of Cajal (ICC) injury [6]. Presently, most of the drugs on the market for the treatment of DGP are chemicals that regulate gastric motility, such as cisapride and metoclopramide. These have limited effects and are further associated with severe side effects [7,8]. Therefore, finding effective natural medicines that can act as alternatives or supplements in the treatment of DGP has become a focus area of current research. In recent years, several scholars have reported on the immense potential of different natural Chinese medicines, such as *Coptidis Rhizoma* and *Pinelliae Rhizoma*, in the treatment of DGP [9–11]. Further to these reports, it is important to explore the mechanisms of DGP and develop novel strategies toward preventing and treating medical conditions from the perspective of Traditional Chinese Medicine (TCM).

Alpinia officinarum Hance (AOH), a species of ginger in the ginger family, is a dried rhizome that serves as a Chinese herbal medicine. It is used both as a food and medicine and has a long history in China. AOH is a characteristic Li-medicine widely distributed in the Hainan Province of the country [12]. Additionally, previous pharmacological studies have established that AOH has anti-inflammatory, anti-gastric ulcer, antiemetic, and antidiabetic properties. Fur-

thermore, AOH promotes gastric emptying and intestinal propulsion and exerts hypoglycemic, gastrointestinal protection, and other pharmacological activities [13,14]. According to the theory of TCM, AOH has long been considered to have the functions of warming the stomach and halting vomiting, dissipating cold and relieving pain, and strengthening the spleen and stomach, features that are suitable for the treatment of DGP [15]. Hence, AOH has become a key ingredient in various TCM formulations for treating DGP [16,17]. However, to accurately and comprehensively understand the mode of action of AOH in the treatment of DGP, its active ingredients and underlying molecular mechanisms should be explored, which is the focus of this study.

Network pharmacology was first proposed by Andrew L Hopkins in 2007, and it has become one of the hotspots in pharmacology research in recent years [18]. Network pharmacology is a strategy for systematic analysis of the interaction between diseases and drugs and between active ingredients and drug targets. The technique has been widely used as a predictive tool in the field of TCM to explore the possible plan for treating diseases [18]. In addition, molecular docking serves as a method for potential drug design by simulating the binding mode and affinity of drug molecules to the targets in the human body [19]. A previous study has proved that the merging of network pharmacology and molecular docking could accelerate experimental validation and target discovery [20]. Thus, in this work, both studies were performed to explore the potential mechanism of AOH in DGP. Subsequently, a series of experiments have been set-up and are ongoing in DGP mice to confirm the previously predicted mechanism, and we hope that the findings would serve as a reference for treating DGP with TCM.

2. Materials and Methods

2.1 Materials and Reagents

Male C57BL/KsJ db/db and db/m mice aged 8 weeks were purchased from Jiangsu Jicui Yaokang Biotechnology Co., Ltd (Nanjing, China). The following materials and reagents were used in this study: AOH granule (GaoliangjiangPeifangkeli) was purchased from Guangdong Yifang Pharmaceutical Co., Ltd (No.: 1045051, Foshan, China); Indocyanine Green (No.: 1I2633) and D-(+)-Glucose (No.: G8270) were purchased from Sigma (St. Louis, MO, USA); Phenol red was purchased from Shanghai Yuanye Bio-Technology Co., Ltd (No.: S19017, Shanghai, China); Eastep®Super Total RNA Extraction Kit was from Shanghai Promage Biological Products Co., Ltd (No.: LS1040, Shanghai, China); Phenylmethylsulfonyl fluoride (PMSF) was from Aladdin (No.: L913093, Shanghai, China); RIPA Lysis Buffer (No.: P0013C) and BCA Protein Assay Kit (No.: P0011) were purchased from Beyotime (Shanghai, China); PI3K polyclonal antibody (No.: #4257), phospho-PI3K (pPI3K, No.: #17366), AKT polyclonal antibody (No.: #4691), phospho-AKT (pAKT, No.: #4060), and anti-Rabbit IgG, HRP-linked antibody (No.: #7074) were purchased from Cell Signaling Technology (Danvers, MA, USA), and anti-GAPDH was from Proteintech (No.: #62u0922, Chicago, IL, USA); MTL (No.: H182), MDA (No.: A003-1), and SOD (No.: A001-3) were purchased from Nanjing Jiancheng Bioengineering Institute (Nanjing, China).

2.2 Network Pharmacology Method Construction

2.2.1 Screening of Active Compounds and Targets of AOH

Traditional Chinese Medicine Systems Pharmacology Database and Analysis Platform (TCMSP, https://old.tcmsp-e.com/tcmsp.php) was employed to search all herbal components of AOH [21]. Next, the drug absorption, distribution, metabolism, and excretion (ADME) parameters were applied to screen the potential active ingredients with an Oral Bioavailability (OB) $\geq$30% and Drug-Likeness (DL) $\geq$0.18 set as the main indicators.

Then, TCMSP and SwissTargetPrediction databases (http://www.swisstargetprediction.ch/) were employed to search for targets corresponding to the AOH active ingredients [22,23]. The Uniprot database (https://www.uniprot.org/) [24] was used to set species as "*Homo sapiens*" and convert the target proteins to matching target genes. Finally, a database of AOH compounds and their targets was constructed.

2.2.2 Differential Gene Screening for DGP—Screening of Clinical Differential Genes

The proteomic expression data of DGP patients and non-diabetic non-gastroparetic controls were retrieved from the GEO database of the National Center for Biotechnology Information (NCBI) (https://www.ncbi.nlm.nih.gov/geo/, GSE130672; GPL23119, 14 samples) with $p < 0.05$ and $|\log2 \text{ (fold change)}| > 1$, which were considered as target genes with a significant expression difference in DGP patients and with research value [25].

2.2.3 Differential Gene Screening for DGP—Screening of Other Differential Genes

"Diabetic gastroparesis" was used as the keyword to screen the related genes from the following databases: GeneCards database (https://www.genecards.org) [26], Pharmacogenetics and Pharmacogenomics Knowledge Base (PharmGKB) database (https://www.pharmgkb.org/) [27], Therapeutic Target Database (TTD) (http://db.idrblab.net/ttd/) [28], DrugBank database (https://www.drugbank.ca/) [29] and the Online Mendelian Inheritance in Man (OMIM) database (https://www.omim.org/) [30]. Furthermore, the obtained data were combined and the duplicate entries were removed. Finally, the Venn diagram (http://bioinformatics.psb.ugent.be/webtools/Venn/) was applied to visualize the ultimate results.

2.2.4 Potential Targets for the Intersection of AOH with DGP

The predicted targets of active ingredients of AOH and the targets related to DGP were depicted in a Venn diagram, with the overlapping portion denoting the common targets of AOH and DGP.

2.2.5 Protein–Protein Interaction (PPI) Analysis

The common targets of disease and drug obtained above were imported into the Search Tool for the Retrieval of Interacting Genes/Proteins (STRING) 11.0 (https://string-db.org) [31], and the species column was selected as "*homo sapiens*". Medium confidence = 0.4 was set as the lowest interaction score, and the rest of the settings were maintained at their default values. The PPI data were collected, collated, and imported into the Cytoscape 3.7.2 program [32] to construct the PPI network diagram. Subsequently, the degree, betweenness, and closeness in the CytoNCA analysis [33] were used to screen the network for primary targets.

2.2.6 Gene Ontology (GO) and Kyoto Encyclopedia of Genes and Genomes (KEGG) Pathway Enrichment Analysis

To determine the specific targets and pathways of AOH that improve DGP, GO functional analysis and KEGG pathway enrichment analysis were conducted with reference to the Metascape database (http://metascape.org/gp/index.html) [34]. The results revealed that Biological Process (BP), Cellular Component (CC), Molecular Function (MF), and signaling pathways were closely associated with improvement of DGP by AOH.

2.2.7 Construction of Network of "component–target–pathway"

The previously screened AOH active components, common targets, and main signaling pathways were imported into the Cytoscape 3.7.2 software (https://cytoscape.org/release_notes_3_7_2.html), and the "component–target–pathway" (C–T–P) network of AOH to ameliorate DGP was constructed. The "C–T–P" network comprised nodes and edges, wherein the nodes represented the major pharmacodynamic compounds of AOH, potential targets, and key pathways that acted concertedly, and the edges represented intermolecular interactions and mainly referred to the association between the active ingredients and key targets and signaling pathways.

2.3 Construction of Molecular Docking Simulation Method

According to the magnitude of the degree value obtained in network pharmacology analysis, the structures of the top five components (quercetin, kaempferol, medicarpin, galangin, and 1,7-diphenyl-5-hydroxy-3-heptanone) were painted in Discovery Studio 2019 [35]. The crystal structure of key proteins in the PI3K-AKT signaling pathway, namely, AKT1 (PDB ID: 6HHI) and PIK3CA (PDB ID: 6AUD), were obtained from the RCSB database (http://www.RCSB.org) [36]. The proteins were placed in Discovery Studio 2019 to remove water molecules and ligands from the environment. Then, polar hydrogen atoms were added, and their docking site and binding capacity of the ligand and protein were recorded.

2.4 In Vivo Validation Experiments

2.4.1 Model Establishment, Grouping, and Administration

Male C57BL/KsJ db/db and db/m mice (aged 8 weeks) were purchased from Jiangsu Jicui Yaokang Biotechnology Co., Ltd., China. The mice were housed at a temperature of 25 °C and a humidity of 50%–65%, with 12-h light/dark cycles, and had free access to standard water and laboratory diets. All animal experiments were approved by the Experimental Animal Ethics Committee of Hainan Medical University (Permit No. HYLL-2021-377).

After 1 week of adaptive feeding, the DGP mouse model was constructed by modifying a previously reported method [37]. Eight db/m mice constituted the control group and were regularly fed with chow diet, and sixteen db/db mice were fed a high-fat diet (HFD, 60% fat, 20% protein, and 20% carbohydrate) in an irregular manner (fasted on odd days, fed on even days) to promote the development of DGP [38]. During DGP modeling, AOH (75 mg/kg) was administered to prevent the development of DGP. Briefly, the mice were randomly categorized into three groups (n = 8), as follows: (1) control (CON) group; (2) DGP group; and (3) AOH group. The AOH was dissolved in distilled water and administered via oral gavage at a dose of 0.2 mL/10 g once a day for 9 weeks. The mice in the CON and DGP groups were given the same physiological volume of distilled water. During the experiments, fasting blood glucose (FBG, fasting for 8 h) and body weight were monitored and recorded weekly.

2.4.2 Fluorescence Imaging to Visualize Gastric Emptying

Gastric emptying was visualized by slightly modifying a previous study protocol [39]. In the 6th week of treatment, the mice were depilated before the initiation of fluorescence imaging. The mice were fasted for 12 h, and 100 μL of orally gavaged indocyanine green was administered at a concentration of 1 mg/mL. Subsequently, the animals were anesthetized with isoflurane, and live images were obtained using IVIS Lumina XR (Perkin Elmer, Excitation: 780 nm, Emission: 831 nm, Waltham, MA, USA). Finally, fluorescence intensities in the mice at different time points (5 min, 30 min, and 50 min) were monitored.

2.4.3 Sample Collection and Determination of Biochemical Indicators

One week before the end of the animal experiment, an oral glucose tolerance test (OGTT) was conducted. Briefly, after fasting for 12 h in each group, the blood glucose levels were measured at 0, 15, 30, 60, and 120 min after administering 2 g/kg of glucose. Finally, the glucose level was plotted as a curve, and the area under the curve (AUC) of OGTT was calculated.

All mice were euthanized in the 9th week of treatment, and the blood and stomach were collected after dissecting the mice. The blood samples were allowed to stand at room temperature for 2 h and then centrifuged at 3500 rpm for 15 min to obtain the serum. The stomach tissues were collected and stored at –80 °C for Western blotting (WB) and quantitative polymerase chain reaction (qPCR) analysis.

An automatic biochemistry analyzer was used to analyze the serum biochemical parameters, including total cholesterol (TC), triglyceride (TG), and alanine aminotransferase (ALT) levels. Serum motilin (MTL), malonic dialdehyde (MDA), and superoxide dismutase (SOD) levels were measured according to the instructions in the enzyme-linked immunosorbent assay (ELISA) kit.

2.4.4 Detection of the Liquid Gastric Emptying Rate

Gastrointestinal propulsion was detected using the phenol red method as previously described [40]. Before euthanasia, the mice were treated orally with 300 µL of phenol red solution (0.05% w/v phenol red suspension in 1.5% w/v suspension of carboxymethylcellulose). After another 20 min, the mice were sacrificed and the entire stomach was carefully isolated and ligated just above the cardia and below the pylorus and separated. Its contents were poured into a beaker and washed with 20 mL of 0.9% normal saline. Subsequently, the contents were added to 20 mL of 0.5 mol/L NaOH, and 4 mL of trichloroacetic acid (20% w/v) was added for deproteinization. The absorbance of the supernatant was read at 560 nm using a Molecular Devices Spectra Max Plus automatic plate reader (Molecular Device, Sunnyvale, CA, USA) after centrifugation (3500 rpm for 10 min). Next, 18 mL of distilled water, 20 mL of 0.5 mol/L NaOH, and 4 mL of trichloroacetic acid (20% w/v) were added to 2 mL of phenol red solution and mixed well to measure the absorbance as a blank control. The gastric emptying rate was calculated according to the following equation: gastric emptying rate (%) = (1 – absorbance of phenol red collected from the stomach 20 min after gavage with phenol red/absorbance of blank control) × 100.

2.4.5 qPCR Analysis

According to the manufacturer's instructions, total RNA was isolated from gastric tissues using the Eastep®Super Total RNA Extraction Kit. Later, a single-stranded cDNA was synthesized from 2 µg of total RNA using reverse transcriptase. Afterward, quantitative polymerase chain reaction (qPCR) was performed using the following amplification conditions: a precycling stage at 95 °C for 5 min, followed by 40 cycles of the second step (i.e., denaturing at 95 °C for 10 sec, annealing at 60 °C for 20 sec, and elongation at 72 °C for 20 sec). Ultimately, nonspecific amplifications were monitored with the melting curves, and the $2^{-\Delta\Delta Ct}$ method was used to analyze the relative expression of mRNA. The relative expression abundance of all genes was normalized with GAPDH. The primer sequences used for qPCR are presented in Table 1.

Table 1. The primer sequences of qPCR.

Primer	Primer sequence (5′ to 3′)
PI3K-F	GTGGTAGATGGCGAAGTCA
PI3K-R	CAGGGAGGTGTGTTGGTAA
AKT-F	GCTGGAGAACCTCATGCTG
AKT-R	GTGTCCCGCAGAACGTC
GAPDH-F	CCTTCCGTGTCCCCACT
GAPDH-R	GCCTGCTTCACCACCTTC

qPCR, quantiative polymerase chain reaction.

2.4.6 WB Analysis

Gastric tissues were homogenized on ice and centrifuged at 15,000 rpm for 10 min at 4 °C after weighing them and cutting them with scissors. The total protein was extracted from the mice's gastric tissue using radioimmunoprecipitation assay (RIPA) lysis buffer in each group, and protein concentrations were measured using the bicinchoninic acid protein assay kit. Protein samples were mixed with 5× loading buffer and denatured at 100 °C for 5 min. Then, gel preparation and sample loading were performed. Subsequently, the proteins in the gel were transferred to a polyvinylidene difluoride membrane by wet transfer after electrophoretic separation. The membranes were blocked with 5% skim milk powder in Tris-buffered saline with 0.1% Tween 20 blocking solution for 1 h. After the membrane was washed, it was incubated with PI3K (1:1000), AKT (1:2000), p-PI3K (1:1000), p-AKT (1:2000), and GAPDH (1:10,000) overnight at 4 °C. After washing, the membrane was incubated with secondary antibodies for 1 h at room temperature. Eventually, images were analyzed, and relative expression levels of proteins were determined using the Image Lab analysis software (Bio-Rad Laboratories, Inc., Hercules, CA, USA). GAPDH served as the internal reference.

2.5 Statistical Analysis

All data were presented as mean ± standard deviation (mean ± SD). Statistical analysis was performed using the GraphPad Prism 8.0.2 software (GraphPad Software, San Diego, CA, USA), and $p < 0.05$ was considered statistically significant.

Table 2. Detailed information on the 13 active components from AOH.

MOL ID	Molecule name	Structure	OB (%)	DL
MOL001771	Poriferast-5-en-3beta-ol	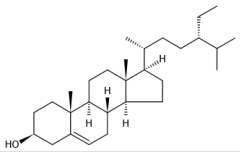	36.91	0.75
MOL002543	(2S,3R)-2-(3,4-dimethoxyphenyl)-5,7-dimethoxychroman-3-ol	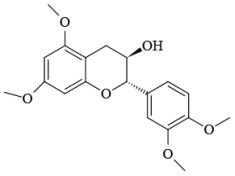	51.89	0.37
MOL002544	1,7-diphenyl-5-hydroxy-3-heptanone	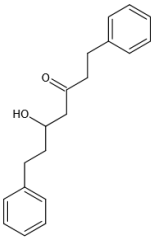	61.9	0.18
MOL002554	5-methoxy-1,7-diphenyl-3-heptanone	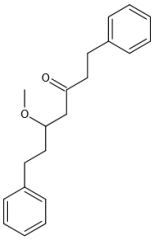	68.29	0.20
MOL002556	7-Methoxy-8-(2′-ethoxy-3′-hydroxy-3′-methybutyl)coumarin	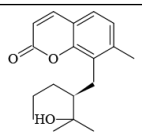	40.36	0.21
MOL002563	Galangin	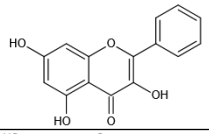	45.55	0.21
MOL002565	Medicarpin	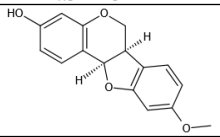	49.22	0.34
MOL002575	Butyl-2-ethylhexyl phthalate	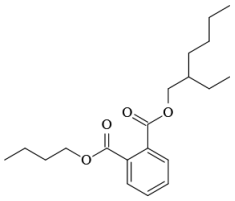	44.52	0.22
MOL000354	Isorhamnetin	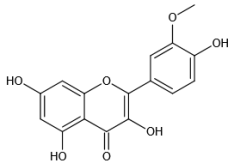	49.6	0.31
MOL000358	Beta-sitosterol	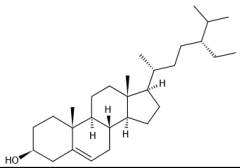	36.91	0.75

Table 2. Continued.

MOL ID	Molecule name	Structure	OB (%)	DL
MOL000359	Sitosterol	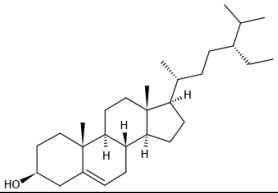	36.91	0.75
MOL000422	Kaempferol	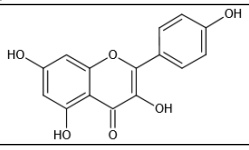	41.88	0.24
MOL000098	Quercetin	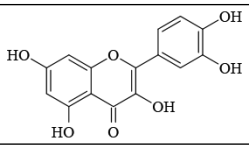	46.43	0.28

3. Results

3.1 Network Pharmacology Prediction

3.1.1 Information on Active Compounds and Targets of AOH

Searching the TCMSP database revealed that 130 compounds were currently known to be found in AOH. Subsequently, 13 active compounds were screened across all compounds based on two key ADME parameters (OB $\geq$30% and DL $\geq$0.18) (Table 2). In addition, the TCMSP and SwissTargetPrediction databases were used to obtain the targets corresponding to the active components of AOH, and finally 498 targets were obtained (**Supplementary Table 1**).

3.1.2 Analysis of Differential Genes related to DGP

A total of 136 differentially expressed targets related to DGP were obtained from the GEO database search, of which 76 were downregulated and 60 were upregulated (Fig. 1A,B).

In addition, using "diabetic gastroparesis" as the keyword, a total of 674 possible candidate targets were screened from different databases, including 581 in GeneCards, 38 in PharmGKB, 5 in TTD, 14 in DrugBank, and 61 in OMIM (Fig. 1C).

3.1.3 Potential Targets of AOH for Improving DGP

Venn analysis of 498 targets of AOH active components and 674 DGP-related targets resulted in the identification of 89 drug–disease intersection targets, which were important targets that played a key role in the alleviation of DGP by AOH (Fig. 1D).

3.1.4 Establishment of the PPI Network

The 89 drug–disease intersection gene targets obtained above were imported into the STRING database, where reliable interaction information could be predicted and imported into Cytoscape for analysis and construction of PPI networks. After hiding the unconnected nodes, a PPI network comprising 88 nodes and 2517 edges was obtained. The larger the node, the greater its biological functions in the PPI network (Fig. 1E). Therefore, according to the results of degree, betweenness, and closeness, 13 key nodes were further screened out and defined as the "key targets" for subsequent research. The degree values of the 13 most closely related target proteins are presented in Fig. 1F.

3.1.5 GO and KEGG Pathway Enrichment Analyses

The results indicated that the enriched BPs were mainly responses to xenobiotic stimulus, positive regulation of protein phosphorylation, transferase activity and MAPK cascades, regulation of kinase and protein kinase activity, and cellular responses to various types of compounds; the enriched CCs were mainly related to membrane raft, micromembrane domain, and synaptic composition; and the enriched MFs were predominantly related to kinase activity, protein phosphatase binding, cytokine receptor binding, and transcription factor binding (Fig. 1G).

Furthermore, the KEGG pathway enrichment analysis was used to decipher the potential role of signaling pathways. Of the 91 signaling pathways, the top 20 differentially expressed pathways were identified under the screening condition of ascending *p*-value sorting, and the enrichment situation was visually displayed using the enrichment bubble chart. The analysis revealed that the related signaling pathways of AOH for improving DGP chiefly included the PI3K-AKT, AGE-RAGE in diabetic complications, HIF-1, FoxO, p53, and TNF signaling pathways (Fig. 1H).

3.1.6 Construction of the Network of "component–target–pathway"

To further investigate the potential molecular mechanism of AOH in improving DGP, a "component–target–pathway" network was constructed based on the top 20 sig-

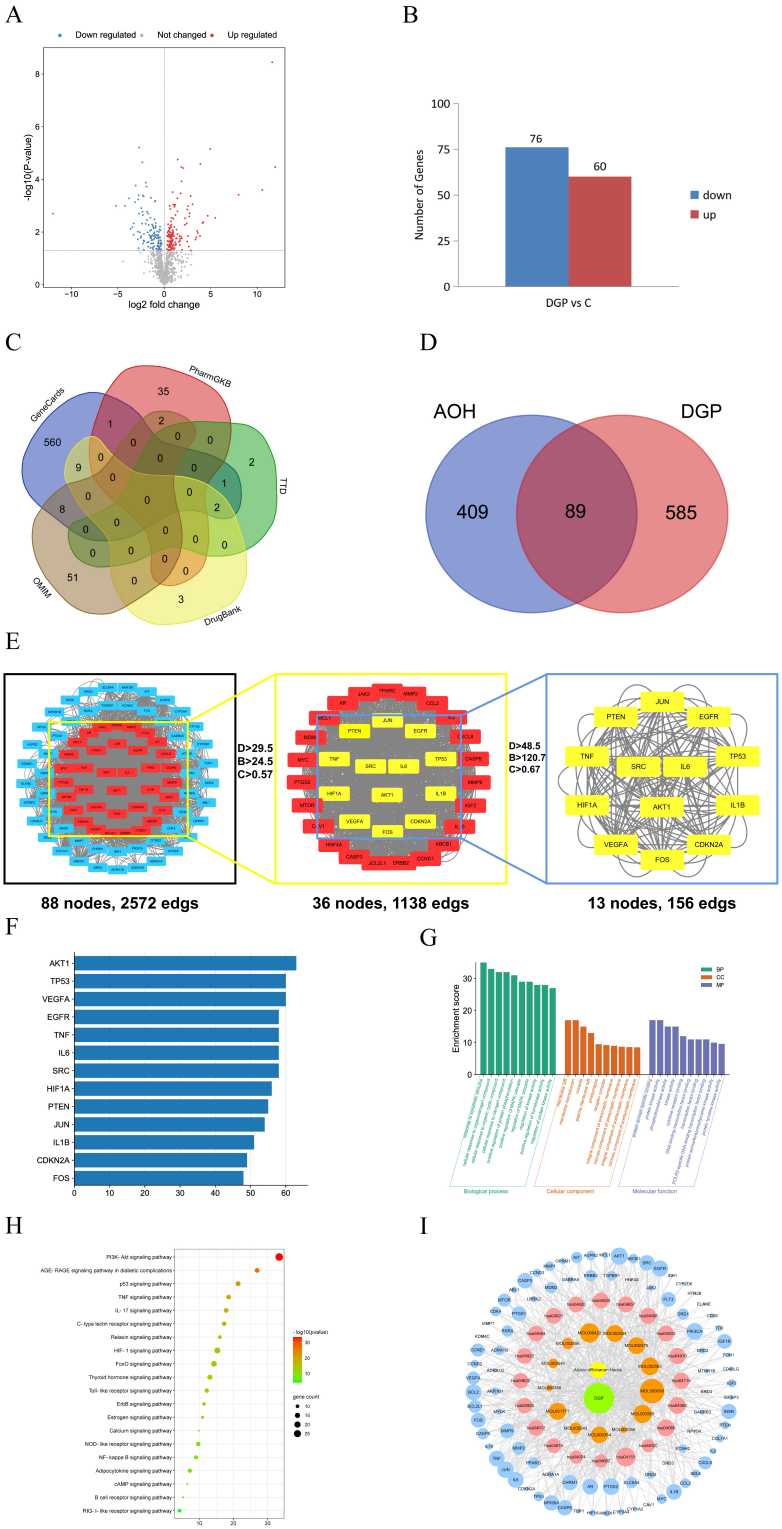

Fig. 1. Network pharmacology analyses of AOH on DGP. (A) A volcano map of differentially expressed genes in DGP patients (The abscissa represents the fold changes in gene expression, and the ordinate represents the statistical significance of the gene expression change). (B) The number of differential genes in DGP patients (DGP stands for DGP patients; C stand for non-diabetic non-gastroparetic controls). (C) Venn diagram of differentially expressed genes in DGP. (D) Venn diagram and candidate targets of AOH and DGP. (E) PPI network (D, Degree; B, Betweenness; C, Closeness). (F) Degree values of the top 13 target proteins. (G) GO enrichment analysis of targets of AOH. (H) Analysis of KEGG enrichment in 20 pathways as targets of AOH. (I) "component-target-pathway" of AOH ameliorating DGP (Blue nodes: overlapping genes between AOH and DGP; pink nodes: the KEGG pathway; orange nodes: the active ingredients of AOH). AOH, *alpinia officinarum* hance; DGP, diabetic gastroparesis; PPI, protein–protein interaction; GO, Gene Ontology; KEGG, Kyoto Encyclopedia of Genes and Genomes.

Table 3. Docking Analysis of the Target Proteins and Compounds.

Target Proteins	Compound	CDocker energy	CDocker interaction energy	Interacting residues
AKT1	Quercetin	–35.7211	–42.6291	GLU A:85, lLE A:84, THR A:82, LYS A:179, ASP A:292, PHE A:293, GLY A:294, TYR A:272, THR A:272, ASP A:274, VAL A:271, VAL A:270, ASN A:54, GLN A:79, ARG A:273, TYR A:326
	Kaempferol	–33.2075	–39.4437	ILE A:84, THR A:82, ASP A:274, GLY A:293, ASN A:279, PHE A:293, TYR A:272, THR A:291, ASP A:292, VAL A:271, VAL A:270, ASN A:54, GLN A:79, ARG A:273
	Medicarpin	–7.24454	–33.5406	ILE A:84, TYR A:326, VAL A:271, ARG A:273, ASN A:54, GLN A:79, THR A:82, ASP A:292, LYS A:179, GLY A:294, ASP A:274, TYR A:272, TYR A:18, GLU A:85, GLU A:17, ARG A:86
	Galangin	–27.5689	–32.966	THR A:81, TRP A:80, THR A:82, GLN A:79, ASN A:54, ARG A:273, GLU A:17, TYR A:18, ILE A:84, ASP A:274, TYR A:272, THR A:291, ASP A:292
	1,7-diphenyl-5-hydroxy-3-heptanone	–37.8872	–38.5737	LEU A:295, CYS A:310, LYS A:179, GLY A:294, THR A:82, ASP A:274, TYR A:18, TYR A:272, ILE A:84, ASP A:292, ARG A:273, GLN A:79, ASN A:54, VAL A:270, VAL A:271, VAL A:83, GLU A:85, CYS A:296
PIK3CA	Quercetin	–34.7654	–38.6922	PRO A:789, ARG A:690, TRP A:201, GLN A:291, HIS A:295, LYS A:298, GLU A:852, PRO A:866, ARG A:849, GLU A:880, TYR A:867, GLY A:868, TYR A:787, ASP A:788, PHE A:694
	Kaempferol	–28.3112	–33.7402	ARG A:690, TRP A:201, HIS A:295, GLN A:291, LYS A:298, LEU A:864, GLU A:852, LEU A:865, PRO A:866, ARG A:849, TYR A:867, GLY A:868, GLU A:880, TYR A:787, ASP A:788
	Medicarpin	–6.86184	–33.7583	ARG A:690, HIS A:295, GLU A:852, LYS A:298, LEU A:864, LEU A:865, PRO A:866, TYR A:867 ,GLU A:880, ARG A:849, GLY A:868, TYR A:787, PHE A:694
	Galangin	–23.9584	–29.0952	ASP A:788, ARG A:849, PHE A:694,ARG A:690, TRP A:201, GLN A:291, HIS A:295, LYS A:298, GLU A:852, PRO A:866, TYR A:867, GLU A:880, GLY A:868, TYR A:787
	1,7-diphenyl-5-hydroxy-3-heptanone	–37.459	–40.7001	GLN A:291, TRP A:292, TRP A:201, ASP A:788, GLY A:790, PRO A:789, ARG A:690, GLU A:880, PHE A:694, TYR A:867, LEU A:865, PRO A:866, ARG A:849, GLY A:868, TYR A:787, ARG A:277, HIS A:295

nificant signaling pathways and their corresponding targets (Fig. 1I). The network contained 124 nodes (1 plant, 13 active ingredients, 89 targets, 20 signaling pathways, and 1 disease) and 575 edges. The size of a node was proportional to its topological score in the network; the higher the degree value, the larger the node, and the lower the degree value, the smaller the node. Therefore, the top five active ingredients (quercetin, kaempferol, medicarpin, galangin, and 1,7-diphenyl-5-hydroxy-3-heptanone) were screened according to the size of the nodes in the network, which were considered to be the most likely compounds effective in the treatment of DGP.

3.2 Analysis of Molecular Docking

The aforementioned network pharmacology results revealed that AKT1 is the key target of alleviating DGP by AOH, and AOH may improve DGP via the PI3K-AKT signaling pathway. Hence, the five important components of AOH screened from the TCSMP database were subjected to molecular docking with the core target of the PI3K-AKT signaling pathway (AKT1 and PIK3CA). The combination of small and large molecules is mainly evaluated based on binding energy; when the binding energy is <0, the ligand and the receptor can bind freely [41]. As shown in Table 3, the active ingredients of AOH had high affinities for AKT1 and PIK3CA. The corresponding binding energies were both <0, which further proved the strong binding ability.

The docking results are shown in Fig. 2. The interaction between the ligand and the receptor mainly included van der Waals, conventional hydrogen bond, and carbon-hydrogen bond, of which the conventional hydrogen bond was considered to be the main factor for the formation of protein–drug complexes. The results suggest that the five important compounds of AOH could form at least one conventional hydrogen bond with all active sites (AKT1 and PIK3CA), including ARG-273, GLN-79, VAL-271, TYR-272, THR-291, and GLY-294. In conclusion, the molecular docking simulation results showed that the binding of active ingredients and core targets exhibited a stable point docking structure, which had a structural basis for exerting a certain biological activity and had a certain research value. This result further validated the findings of network pharmacology, i.e., the PI3K-AKT signaling pathway may be connected to AOH, thereby improving DGP.

3.3 In Vivo Experimental Verification

3.3.1 Effects of AOH on FBG Level in DGP Mice

Over time, symptoms of lethargy, polydipsia, polyuria, loose stools, and abdominal distension were observed in DGP mice. Additionally, throughout the experiment, FBG levels of mice in each group were evaluated at a fixed time point every week. The alterations in FBG levels in each group are shown in Fig. 3A. In the CON group, the FBG level remained at a relatively stable

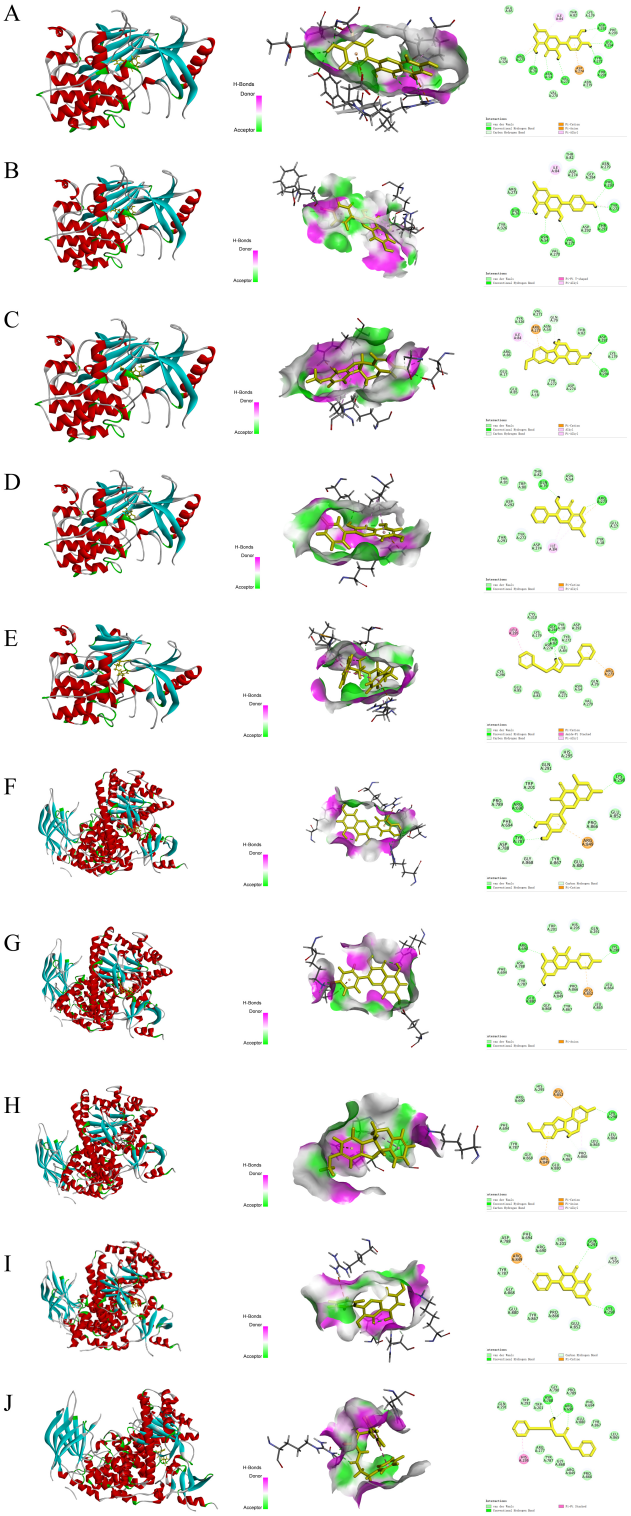

Fig. 2. Molecular docking diagram. (A) AKT1 - Quercetin. (B) AKT1 - Kaempferol. (C) AKT1 - Medicarpin. (D) AKT1 - Galangin. (E) AKT1 - 1,7-diphenyl-5-hydroxy-3-heptanone. (F) PIK3CA - Quercetin. (G) PIK3CA - Kaempferol. (H) PIK3CA - Medicarpin. (I) PIK3CA - Galangin. (J) PIK3CA - 1,7-diphenyl-5-hydroxy-3-heptanone.

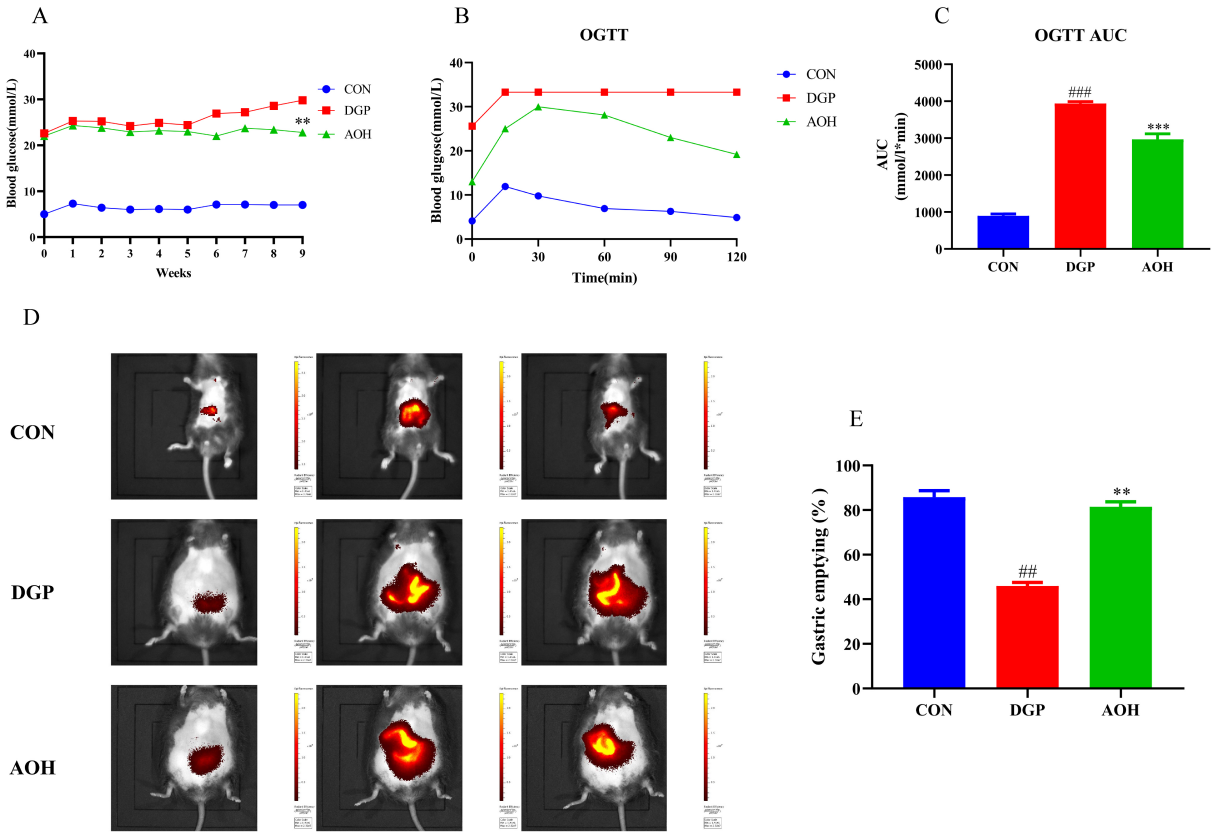

Fig. 3. The effects of AOH on Blood Glucose and Gastric Emptying in DGP Mice. (A) FBG levels. (B) OGTT. (C) The AUC of the OGTT. (D) Fluorescence imaging. (E) Gastric emptying. All values are expressed as the means ± SD (n ≥ 3). ##$p < 0.01$, and ###$p < 0.001$, when compared with the CON group; and **$p < 0.01$, and ***$p < 0.001$, when compared with the DGP group. FBG, fasting blood glucose; OGTT, oral glucose tolerance test.

and normal level throughout the experimental period. However, compared with the CON group, the FBG levels of the DGP and AOH groups increased continuously, with the uptrend of the AOH group being more gradual than that of the DGP group. Moreover, compared with the DGP group, the FBG level was significantly decreased in AOH-treated mice after 9 weeks of drug administration ($p < 0.01$).

OGTT was performed in different groups, and the corresponding AUCs were also analyzed. As shown in Fig. 3B,C, the results of OGTT were ameliorated to some extent in the AOH group. The AUC of the DGP group was significantly higher than that of the CON group ($p < 0.001$) according to the calculation, and the AUC of the AOH group was significantly lower than that of the DGP group ($p < 0.001$) but could not reach the glucose tolerance level of the CON group.

3.3.2 Effects of AOH on Gastric Emptying in DGP Mice

Real-time ICG fluorescence imaging results are depicted in Fig. 3D. The symptoms of gastroparesis in the mice were judged by the intensity and location of the fluorescence. The mice in the DGP group showed delayed gastric emptying compared with those in the CON group. Administration of AOH, however, significantly accelerated gastric emptying. As expected, the liquid gastric emptying test validated this result (Fig. 3E). Compared with the CON group, the gastric emptying rate decreased significantly in the DGP group ($p < 0.01$), thereby suggesting that the DGP model was established successfully. Furthermore, compared with the DGP group, the gastric emptying rate was increased significantly in the AOH group ($p < 0.01$). The above results demonstrate that AOH significantly promoted gastric emptying in DGP mice, exhibiting a definite alleviating effect.

3.3.3 Effects of AOH on Biochemical Indicators in DGP Mice

The results of serum biochemical assays are displayed in Fig. 4. In Fig. 4A,B, there was a significant increase in the levels of TC and TG in the DGP group compared with the CON group. In contrast, the TC and TG levels were decreased in the serum after AOH treatment ($p < 0.001$). The ALT activity of the DGP group showed a nearly two-fold increase compared with that of the CON group ($p < 0.001$, Fig. 4C), which implied that the liver function of the mice in the DGP group was also affected. Unfortunately, AOH could not effectively improve liver function.

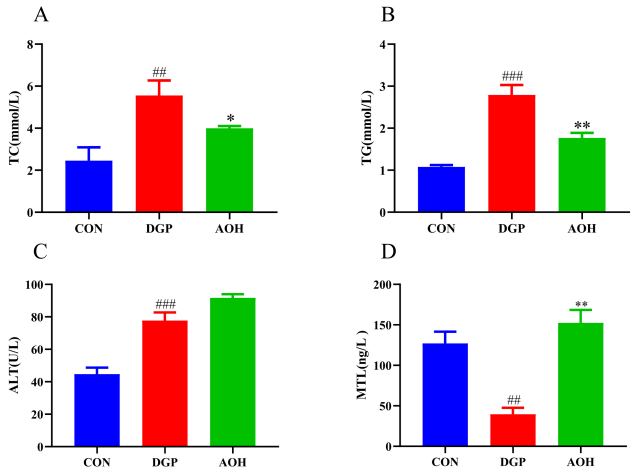

Fig. 4. Effects of AOH on Biochemical Indicator in DGP Mice. (A) TC. (B) TG. (C) ALT. (D) MTL. All values are expressed as the means ± SD, (n ≥ 3). ##$p < 0.01$, and ###$p < 0.001$, when compared with the CON group; and *$p < 0.05$, and **$p < 0.01$, when compared with the DGP group. TC, total cholesterol; TG, triglyceride; ALT, alanine amino-transferase levels; MTL. Serum motilin.

MTL accelerates gastric emptying and is released during the digestive interval [42]. The levels of MTL in different groups were detected using the MTL kit, and the results are presented in Fig. 4D. The MTL level in the DGP group was 3.2 times lower than that in the CON group ($p < 0.01$), which indicated that severe delayed gastric emptying had occurred in the DGP group because of the irregular high-fat diet. However, after the AOH intervention, the MTL level was significantly higher than that of the DGP group ($p < 0.01$), which again proved that AOH can protect the DGP mice from delayed gastric emptying.

These results indicate that AOH could effectively improve the pathological indicators related to type 2 diabetes and further reduce the delayed gastric emptying induced by the disease. However, the molecular mechanism of AOH in ameliorating DGP remains unclear. Hence, we attempted to explore the potential molecular mechanism.

3.3.4 Effects of AOH on the PI3K-AKT Signaling Pathway in DGP Mice

Based on the results of network pharmacology and molecular docking analysis, we discovered that AOH may play a role in the treatment of DGP by regulating the PI3K-AKT signaling pathway, in which PI3K and AKT are the key proteins. Therefore, to further evaluate the molecular mechanisms by which AOH ameliorates DGP, WB and PCR were performed to examine the related targets of AOH. As demonstrated in Fig. 5A–C,E–G, the expressions of AKT and PI3K were significantly lower in the DGP group compared with those in the CON group ($p < 0.01$). However, AOH significantly reversed this decrease in the expression ($p < 0.01$). Furthermore, compared with the DGP group, the phosphorylation of PI3K and AKT was promoted in the AOH group. Moreover, the mRNA expressions of PI3K and AKT were confirmed by this result (Fig. 5D,H), which indicated that AOH might exert its therapeutic effects by regulating the PI3K-AKT signaling pathway.

3.3.5 Effects of AOH on Oxidative Stress in DGP Mice

Oxidative stress is an important factor in the development of DGP, and oxidative damage that occurs in many diseases can be improved via the PI3K-AKT signaling pathway [43–45]. Therefore, the effect of AOH on oxidative stress in DGP mice was investigated. As shown in Fig. 6A,B, the amount of MDA was higher in the DGP mice and the SOD activity was lower ($p < 0.01$). However, AOH significantly enhanced the SOD activity and reduced the MDA levels in stomach homogenates ($p < 0.05$). These results signify that AOH may regulate the related antioxidant enzymes to combat oxidative stress in DGP mice via the PI3K-AKT signaling pathway.

4. Discussion

DGP is a common gastrointestinal complication in patients with diabetes and is chiefly manifested as delayed gastric emptying due to gastrointestinal motility disorder. DGP has become one of the serious diabetic complications that endanger patient health [46]. At present, some drugs are available in the market for the treatment of DGP, but the commonly used antiemetics and prokinetic drugs have limited long-term use owing to their side effects and the high recurrence rate after drug discontinuation [47,48]. For example, domperidone and cisapride are prone to relapse after discontinuation, and metoclopramide causes various side effects, such as depression and drowsiness [49]. However, based on the theory of TCM, research on Chinese medicines that are mild and are associated with fewer side effects has become an important part of supplementary and alternative treatment for DGP [50]. Hence, it is imperative to find mild and effective Chinese medicines that could alleviate DGP.

AOH is a natural medicinal herb widely distributed in southeastern China, and its dried rhizome could treat stomachache and flatulence [51,52]. Previous studies have mostly focused on the protective effect of AOH on the stomach, and AOH, which is a common ingredient in Chinese medicine for the treatment of gastrointestinal diseases, also has the potential to treat DGP [16,17,53]. Nonetheless, the underlying mechanism by which AOH alleviates DGP has not yet been elucidated. Thus, this study explored the mechanism of action deeply using network pharmacology. The binding ability of the active ingredients in AOH to the key targets was simulated with the use of molecular docking, and additional experiments verified the possible mechanism of AOH improving DGP.

The TCMSP database was initially searched in this study, and 13 active compounds related to AOH in the

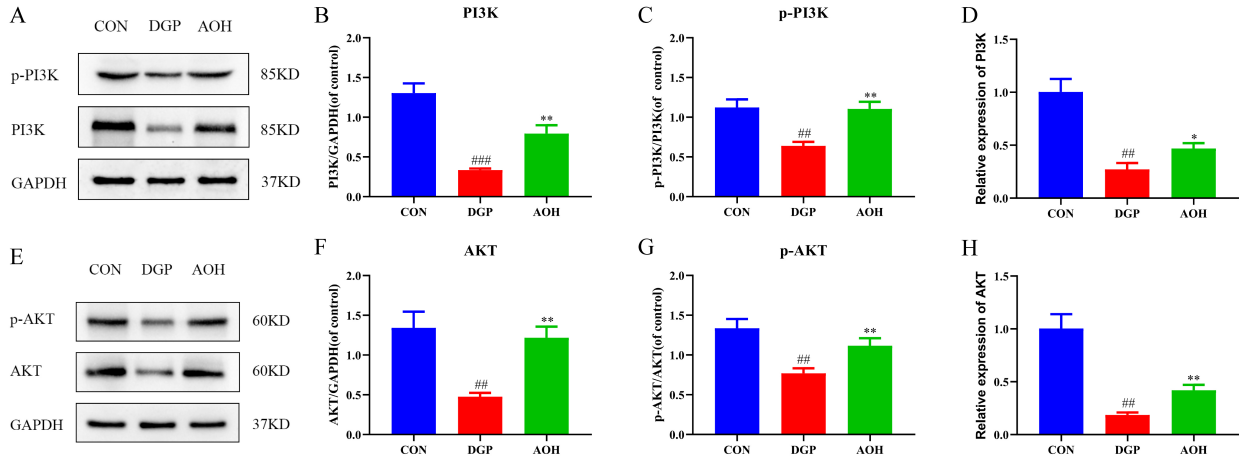

Fig. 5. The effects of AOH on the PI3K-AKT Signaling Pathway in DGP Mice. (A) The protein expression of PI3K and p-PI3K. (B) Quantification of PI3K. (C) Quantification of p-PI3K. (D) mRNA expression of PI3K. (E) Protein expression of AKT and p-AKT. (F) Quantification of AKT. (G) Quantification of p-AKT. (H) mRNA expression of AKT. All values are expressed as the means ± SD ($n \geq 3$). ##$p < 0.01$, and ###$p < 0.001$, when compared with the CON group; and *$p < 0.05$, and **$p < 0.01$, when compared with the DGP group.

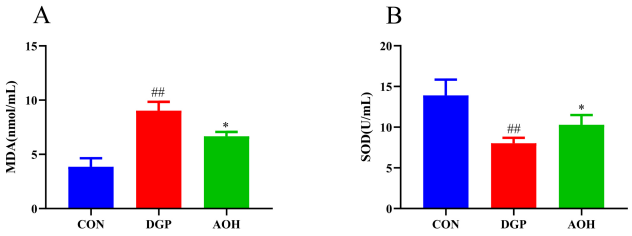

Fig. 6. The effects of AOH on Oxidative Stress in DGP Mice. (A) MDA. (B) SOD. All values are expressed as the means ± SD ($n \geq 3$). ##$p < 0.01$ when compared with the CON group; and *$p < 0.05$, when compared with the DGP group. MDA, malonic dialdehyde.

treatment of DGP were obtained. Subsequently, according to the magnitude of the degree value, quercetin, kaempferol, medicarpin, galangin, and 1,7-diphenyl-5-hydroxy-3-heptanone were proven to be the crucial active ingredients of AOH that acted against DGP. Of these, quercetin, kaempferol, medicarpin, and galangin have been confirmed as natural flavonoids with antioxidant pharmacological activity [54–56]. Moreover, the antioxidant pharmacological activity of these compounds has been shown to aid in the amelioration of DGP [57,58]. On the one hand, quercetin, as the component with the highest coverage of DGP-related targets, has been confirmed to ameliorate the ICC and azinergic neurons in diabetic rats, which is linked to the possible therapeutic mechanism of DGP [59]. On the other hand, quercetin has also been shown to relieve diabetic complications, such as diabetic nephropathy, by attenuating oxidative stress and inflammation. Nevertheless, clinical evidence that it could improve the condition of patients with DGP is lacking [60,61]. In recent years, relevant studies have suggested that kaempferol could improve glucose intolerance and insulin resistance in rodents by inhibiting hepatic gluconeogenesis, increasing insulin sensitivity, and upregulating the level of SIRT1 protein or increasing the activity of AKT and GCK [62–64]. Furthermore, studies have revealed that kaempferol could help treat fibrosis and kidney damage in diabetic rats by activating the Nrf-2/HO-1/antioxidant axis to alleviate diabetic nephropathy [65,66]. Medicarpin is a pterocarpum class of phytoestrogen, which exhibits various biological functions [67]. However, not much research has been conducted to show that medicarpin could treat diabetes or its complications, which may be an emerging research direction in the future. Moreover, galangin, one of the main components of AOH, in addition to its anti-inflammatory and antibacterial effects, could improve insulin resistance and treat diabetes via signaling pathways, such as Akt/mTOR, NF-kappaB p65, and caspase-3 [68–70]. Last but not least, 1,7-diphenyl-5-hydroxy-3-heptanone is a diarylheptanoid compound with pharmacological activities similar to those of flavonoids, namely, anti-inflammatory, antioxidant, and hypoglycemic effects [71,72]. Our previous study confirmed that 1,7-diphenyl-5-hydroxy-3-heptanone could improve type 2 diabetes mellitus via Nrf2/ARE antioxidant elements and PI3K/AKT signaling pathway [72]. Therefore, the active components of AOH listed above indicate its potential effectiveness and diversity in improving DGP. Based on the results of this investigation, the mechanism of action of AOH in the treatment of DGP may be related to its effects on reducing the blood glucose level, enhancing insulin sensitivity, improving the oxidative stress response, and fighting inflammation.

Moreover, 89 potential targets of AOH that act on DGP were identified with Venn analysis, based on which a PPI network was constructed. According to the relevant pa-

rameters, 13 primary targets of AOH that act on DGP were analyzed and screened from the PPI network. The findings suggested the networking of target proteins and their interactions with each other, which are critical for maintaining the physiological balance in the body [11]. As illustrated in Fig. 1, the core proteins embodied in the PPI network were AKT1, IL6, and SRC. Of these, AKT1 was the most important protein and was an antiapoptotic signaling kinase present in various cells. Previous studies have demonstrated that the upregulation of AKT could alleviate DGP symptoms by blocking gastric smooth muscle cell apoptosis and restoring dystonia [37]. To better understand the roles of these target genes and their relationship with each other, KEGG enrichment analysis was performed. The findings revealed that several signaling pathways were significantly associated with the occurrence and progression of DGP. Of the pathways screened, AOH was most likely to exert a therapeutic effect on DGP by regulating the PI3K-AKT signaling pathway. Furthermore, a related study has proved that the PI3K-AKT signaling pathway is one of the key insulin signaling pathways involved in the regulation of glucose and lipid metabolism [73]. Moreover, animal experiments have implied that this pathway may be involved in the treatment of DGP by inhibiting the apoptosis of gastric smooth muscle cells and the loss of gastric antral ICC [38,74].

To validate the reliability of network pharmacology analysis, the main active components and key proteins linked to DGP were selected for molecular docking based on the results of PPI network and KEGG enrichment analysis. The results of molecular docking showed that the active components of AOH screened using network pharmacology could be spontaneously combined with potential targets. Moreover, the binding energy with the core targets, namely, AKT1 and PIK3CA, were all <0. A relatively stable conformation was obtained via interactions such as hydrogen bonds. These results agreed with those from network pharmacology and validated the latter, thereby enhancing the credibility of our research.

For experimental verification, the DGP model was constructed in db/db mice with the method of an irregular high-fat diet, and the anti-DGP effects of AOH were confirmed in this model. In addition, AOH granules were selected as the experimental medicine because they contained the same potent components as conventional decoction pieces and were more convenient to prepare. The chromatograms from HPLC analysis of the main components of AOH granules are shown in **Supplementary Fig. 1**. *In vivo* experimental results established that AOH could ameliorate DGP, including reversing the elevation of FBG level, enhancing gastric emptying rate, and reducing the levels of serum biochemical indicators (TC, TG, and MTL). However, AOH had little effect on the expression of ALT and could not effectively improve liver function. In addition, KEGG enrichment analysis combined with molecular docking indicated that the PI3K-AKT signaling pathway was the most important in improving DGP. Glucose-induced oxidative stress has been postulated to be a key mechanism in chronic diabetic complications, and oxidative damage associated with many diseases could be improved via the PI3K-AKT signal pathway [43–45]. Hence, the effects of AOH on oxidative stress and the PI3K-AKT signal pathway in DGP mice were investigated. Interestingly, AOH effectively regulated the expressions of oxidative stress-related markers (MDA and SOD) in DGP mice via the PI3K-AKT pathway, which agreed with previous studies [71].

In this research, an emerging and efficient method was used for the identification of bioactive ingredients, intersecting targets, and potential mechanisms in the alleviation of DGP by AOH. However, this study has some limitations. First, the data obtained were based on existing databases and simulation tools. As the research on DGP is still in its infancy, the data collected through these databases and tools may have certain inaccuracies. In addition, positive drugs and multiple doses were not used in the experimental verification stage, which needs to be further verified with relevant experiments. Bridging these gaps would be the focus of our team's future work to provide more reliable data supporting the role of AOH in the treatment of DGP.

5. Conclusions

In summary, network pharmacology, molecular docking, and experimental verification were combined to identify the active components, objective targets, and signaling pathways of AOH in the alleviation of DGP. Network pharmacology analysis indicated that quercetin, kaempferol, and galangin, were the potential active components in AOH that acted on the key PI3K-AKT signaling pathway and played a role in the treatment of DGP. Furthermore, molecular docking studies confirmed the above results. Additionally, *in vivo* analysis verified that AOH could regulate the PI3K-AKT signaling pathway against the oxidative stress reaction and alleviate DGP. Collectively, this study not only provides evidence for the therapeutic mechanism of action of AOH against DGP but also points to a key research direction for further experimental studies and clinical applications of AOH.

Availability of Data and Materials

The data used to support the findings of this study are available from the corresponding author upon request.

Author Contributions

XZhe and YZ: Conception and design of experimental ideas, implementation of the whole experimental process, data sorting, writing of the first draft of the manuscript and revision of the final version of the manuscript. JX: provided financial support for research, participated in data analysis and manuscript revision. XL and HW: Implement part of

network pharmacology, molecular docking experiment and data collation. XZha and AL: Implement part of PCR and WB experiment and data collation. JZ: The conception and design of the experimental ideas, funding acquisition, the revision of the final version of the manuscript and guided the whole experimental process. All authors contributed to editorial changes in the manuscript. All authors read and approved the final manuscript. All authors have participated sufficiently in the work and agreed to be accountable for all aspects of the work.

Ethics Approval and Consent to Participate

All animal experiments were approved by the Experimental Animal Ethics Committee of Hainan Medical University (Permit No. HYLL-2021-377).

Acknowledgment

The authors are thankful to Hainan Medical University for the help in conducting this study.

Funding

This research was supported by the Key R&D projects in Hainan Province (ZDYF2022SHFZ305), Natural Science Research Funding "Jie Bang Gua Shuai" Project of Hainan Medical College (JBGS202108), the Major Science and Technology Projects of Hainan Province in 2019 (ZDKJ 2019009) and Hainan Province Clinical Medical Center.

Conflict of Interest

The authors declare no conflict of interest.

Supplementary Material

The targets corresponding to the active components of AOH (**Supplementary Table 1**) and The representative chromatogram of phytochemical compounds in Alpinia officinarum Hance granules (**Supplementary Fig. 1**). Supplementary material associated with this article can be found, in the online version, at https://doi.org/10.31083/j.fbl2808164.

References

[1] Bharucha AE, Kudva YC, Prichard DO. Diabetic Gastroparesis. Endocrine Reviews. 2019; 40: 1318–1352.

[2] Sampath C, Srinivasan S, Freeman ML, Gangula PR. Inhibition of GSK-3β restores delayed gastric emptying in obesity-induced diabetic female mice. American Journal of Physiology. Gastrointestinal and Liver Physiology. 2020; 319: G481–G493.

[3] Gangula PR, Challagundla KB, Ravella K, Mukhopadhyay S, Chinnathambi V, Mittal MK, *et al*. Sepiapterin alleviates impaired gastric nNOS function in spontaneous diabetic female rodents through NRF2 mRNA turnover and miRNA biogenesis pathway. American Journal of Physiology. Gastrointestinal and Liver Physiology. 2018; 315: G980–G990.

[4] Camilleri M, McCallum RW, Tack J, Spence SC, Gottesdiener K, Fiedorek FT. Efficacy and Safety of Relamorelin in Diabetics With Symptoms of Gastroparesis: A Randomized, Placebo-Controlled Study. Gastroenterology. 2017; 153: 1240–1250.e2.

[5] Cerit L, Duygu H. Collapse of the Aspirin Empire: Is it Diabetic Gastroparesis or Cardioprotective Paresis? Journal of the American College of Cardiology. 2017; 69: 2878–2879.

[6] Wang Y, Wang Y, Zhu B, Zhu Y, Jiang Y, Xiong W, *et al*. MALAT1: A Pivotal lncRNA in the Phenotypic Switch of Gastric Smooth Muscle Cells *via* the Targeting of the miR-449a/DLL1 Axis in Diabetic Gastroparesis. Frontiers in Pharmacology. 2021; 12: 719581.

[7] Malamood M, Parkman H, Schey R. Current advances in treatment of gastroparesis. Expert Opinion on Pharmacotherapy. 2015; 16: 1997–2008.

[8] Navas CM, Wadas ED, Zbib NH, Crowell MD, Lacy BE. Gastroparesis and Severity of Delayed Gastric Emptying: Comparison of Patient Characteristics, Treatments and Medication Adverse Events. Digestive Diseases and Sciences. 2021; 66: 526–534.

[9] Liang G, Zhang L, Jiang G, Chen X, Zong Y, Wang F. Effects and Components of Herb Pair Huanglian-Banxia on Diabetic Gastroparesis by Network Pharmacology. BioMed Research International. 2021; 2021: 8257937.

[10] Wang B, Zeng KW, Hong ZF, Ti GX, Wang LY, Lu P, *et al*. Banxia Xiexin Decoction () Treats Diabetic Gastroparesis through PLC-IP_3-Ca^{2+}/NO-cGMP-PKG Signal Pathway. Chinese Journal of Integrative Medicine. 2020; 26: 833–838.

[11] Wu T, Yue R, Li L, He M. Study on the Mechanisms of Banxia Xiexin Decoction in Treating Diabetic Gastroparesis Based on Network Pharmacology. Interdisciplinary Sciences, Computational Life Sciences. 2020; 12: 487–498.

[12] Zhang XG. The study on chemical constituents of Alpinia officinarum in Hainan and the effect on lipids. [Master's thesis]. Hainan Medical University. 2017.

[13] Lin K, Wang Y, Gong J, Tan Y, Deng T, Wei N. Protective effects of total flavonoids from *Alpinia officinarum* rhizoma against ethanol-induced gastric ulcer *in vivo* and *in vitro*. Pharmaceutical Biology. 2020; 58: 854–862.

[14] Gong J, Zhang Z, Zhang X, Chen F, Tan Y, Li H, *et al*. Effects and possible mechanisms of Alpinia officinarum ethanol extract on indomethacin-induced gastric injury in rats. Pharmaceutical Biology. 2018; 56: 294–301.

[15] Yan CX, Shao XM, Wang W. Application of common medicine and food homologous "drug pair" in stomach pain. Chinese Journal of Rural Medicine and Pharmacy. 2020; 27: 17–18.

[16] Li QY, Wei SL, Huang ZG, Nong DX, Liu CY. Diabetic Gastroparesis Randomized Controlled Study of Zhuang Medicine Medicated Thread Moxibustion Therapy combined with Umbilical. Journal of Practical Traditional Chinese Internal Medicine. 2015; 29: 142–144.

[17] Zhang B, Zhang YK, Li HQ. Observation of curative effect on 38 cases of diabetic gastroparesis treated by TCM syndrome differentiation. Shenzhen Journal of Integrated Traditional Chinese and Western Medicine. 2010; 20: 158–159.

[18] Hopkins AL. Network pharmacology. Nature Biotechnology. 2007; 25: 1110–1111.

[19] Abdelsattar AS, Dawoud A, Helal MA. Interaction of nanoparticles with biological macromolecules: a review of molecular docking studies. Nanotoxicology. 2021; 15: 66–95.

[20] Huang J, Zhou X, Gong Y, Chen J, Yang Y, Liu K. Network pharmacology and molecular docking analysis reveals the mechanism of asiaticoside on COVID-19. Annals of Translational Medicine. 2022; 10: 174.

[21] Ru J, Li P, Wang J, Zhou W, Li B, Huang C, *et al*. TCMSP: a database of systems pharmacology for drug discovery from herbal medicines. Journal of Cheminformatics. 2014; 6: 13.

[22] Daina A, Michielin O, Zoete V. SwissTargetPrediction: updated data and new features for efficient prediction of protein targets of small molecules. Nucleic Acids Research. 2019; 47: W357–W364.
[23] Gfeller D, Michielin O, Zoete V. Shaping the interaction landscape of bioactive molecules. Bioinformatics. 2013; 29: 3073–3079.
[24] UniProt Consortium T. UniProt: the universal protein knowledgebase. Nucleic Acids Research. 2018; 46: 2699.
[25] Grover M, Dasari S, Bernard CE, Chikkamenahalli LL, Yates KP, Pasricha PJ, *et al*. Proteomics in gastroparesis: unique and overlapping protein signatures in diabetic and idiopathic gastroparesis. American Journal of Physiology. Gastrointestinal and Liver Physiology. 2019; 317: G716–G726.
[26] Stelzer G, Rosen N, Plaschkes I, Zimmerman S, Twik M, Fishilevich S, *et al*. The GeneCards Suite: From Gene Data Mining to Disease Genome Sequence Analyses. Current Protocols in Bioinformatics. 2016; 54: 1.30.1–1.30.33.
[27] Whirl-Carrillo M, Huddart R, Gong L, Sangkuhl K, Thorn CF, Whaley R, *et al*. An Evidence-Based Framework for Evaluating Pharmacogenomics Knowledge for Personalized Medicine. Clinical Pharmacology and Therapeutics. 2021; 110: 563–572.
[28] Zhou Y, Zhang Y, Lian X, Li F, Wang C, Zhu F, *et al*. Therapeutic target database update 2022: facilitating drug discovery with enriched comparative data of targeted agents. Nucleic Acids Research. 2022; 50: D1398–D1407.
[29] Wishart DS, Feunang YD, Guo AC, Lo EJ, Marcu A, Grant JR, *et al*. DrugBank 5.0: a major update to the DrugBank database for 2018. Nucleic Acids Research. 2018; 46: D1074–D1082.
[30] Amberger JS, Bocchini CA, Scott AF, Hamosh A. OMIM.org: leveraging knowledge across phenotype-gene relationships. Nucleic Acids Research. 2019; 47: D1038–D1043.
[31] Szklarczyk D, Gable AL, Nastou KC, Lyon D, Kirsch R, Pyysalo S, *et al*. The STRING database in 2021: customizable protein-protein networks, and functional characterization of user-uploaded gene/measurement sets. Nucleic Acids Research. 2021; 49: D605–D612.
[32] Otasek D, Morris JH, Bouças J, Pico AR, Demchak B. Cytoscape Automation: empowering workflow-based network analysis. Genome Biology. 2019; 20: 185.
[33] Lotia S, Montojo J, Dong Y, Bader GD, Pico AR. Cytoscape app store. Bioinformatics. 2013; 29: 1350–1351.
[34] Zhou Y, Zhou B, Pache L, Chang M, Khodabakhshi AH, Tanaseichuk O, *et al*. Metascape provides a biologist-oriented resource for the analysis of systems-level datasets. Nature Communications. 2019; 10: 1523.
[35] Kemmish H, Fasnacht M, Yan L. Fully automated antibody structure prediction using BIOVIA tools: Validation study. PloS one. 2017; 12: e0177923.
[36] Berman HM, Westbrook J, Feng Z, Gilliland G, Bhat TN, Weissig H, *et al*. The Protein Data Bank. Nucleic Acids Research. 2000; 28: 235–242.
[37] Zhang XZ, Zhang MH, Fang XS, Cui XS, Jin Z. Mechanism of AMPK-mediated apoptosis of rat gastric smooth muscle cells under high glucose condition. Bioscience Reports. 2019; 39: BSR20192504.
[38] An X, Long C, Deng X, Tang A, Xie J, Chen L, *et al*. Higenamine inhibits apoptosis and maintains survival of gastric smooth muscle cells in diabetic gastroparesis rat model via activating the β2-AR/PI3K/AKT pathway. Biomedicine & Pharmacotherapy. 2017; 95: 1710–1717.
[39] Cai Y, Zheng Z, Gao P, Li Y, Peng B. Laparoscopic duodenum-preserving total pancreatic head resection using real-time indocyanine green fluorescence imaging. Surgical Endoscopy. 2021; 35: 1355–1361.
[40] Ha C, Kim H, Cha R, Lee J, Lee S, Ryu JH, *et al*. Effect of DA-9701 on the Gastrointestinal Motility in the Streptozotocin-Induced Diabetic Mice. Journal of Clinical Medicine. 2021; 10: 5282.
[41] Li X, Wen H, Zhang Y, Liu A, Zhang X, Fu M, *et al*. DPHB, a diarylheptane from *Alpinia officinarum* Hance, ameliorates insulin resistance: A network pharmacology and *in vitro* study. Frontiers in Pharmacology. 2022; 13: 956812.
[42] Sanger GJ, Broad J, Callaghan B, Furness JB. Ghrelin and Motilin Control Systems in GI Physiology and Therapeutics. Handbook of Experimental Pharmacology. 2017; 239: 379–416.
[43] Da Silva LM, da Silva RDCMVDAF, Maria-Ferreira D, Beltrame OC, da Silva-Santos JE, Werner MFDP. Vitamin C Improves Gastroparesis in Diabetic Rats: Effects on Gastric Contractile Responses and Oxidative Stress. Digestive Diseases and Sciences. 2017; 62: 2338–2347.
[44] Ren BC, Zhang YF, Liu SS, Cheng XJ, Yang X, Cui XG, *et al*. Curcumin alleviates oxidative stress and inhibits apoptosis in diabetic cardiomyopathy via Sirt1-Foxo1 and PI3K-Akt signalling pathways. Journal of Cellular and Molecular Medicine. 2020; 24: 12355–12367.
[45] Zhang BH, Liu H, Yuan Y, Weng XD, Du Y, Chen H, *et al*. Knockdown of TRIM8 Protects HK-2 Cells Against Hypoxia/Reoxygenation-Induced Injury by Inhibiting Oxidative Stress-Mediated Apoptosis and Pyroptosis via PI3K/Akt Signal Pathway. Drug Design, Development and Therapy. 2021; 15: 4973–4983.
[46] Wang S, Wang R, Zhang Y, Zhang X, Cai B, Lu Y, *et al*. Therapies for diabetic gastroparesis: A protocol for a systematic review and network meta-analysis. Medicine. 2020; 99: e20461.
[47] Shakhatreh M, Jehangir A, Malik Z, Parkman HP. Metoclopramide for the treatment of diabetic gastroparesis. Expert Review of Gastroenterology & Hepatology. 2019; 13: 711–721.
[48] Camilleri M, Lembo A, McCallum R, Tourkodimitris S, Kemps L, Miller MB, *et al*. Overall safety of relamorelin in adults with diabetic gastroparesis: Analysis of phase 2a and 2b trial data. Alimentary Pharmacology & Therapeutics. 2020; 51: 1139–1148.
[49] Yao J, Peng B, Gong X, Shi X, Fan S, Chen Q. Efficacy and Safety of Mecobalamin Combined with Prokinetic Agents in the Treatment of Diabetic Gastroparesis: A Meta-Analysis. Iranian Journal of Public Health. 2021; 50: 2161–2171.
[50] Pang B, Zhou Q, Li JL, Zhao LH, Tong XL. Treatment of refractory diabetic gastroparesis: Western medicine and traditional Chinese medicine therapies. World Journal of Gastroenterology. 2014; 20: 6504–6514.
[51] Tang X, Xu C, Yagiz Y, Simonne A, Marshall MR. Petrochemical profiles, and antimicrobial and antioxidant activities of greater galangal [Alpinia galanga (Linn.) Swartz.] flowers. Food Chemistry. 2018; 255: 300–308.
[52] Zhou W, Sun Y, Zou L, Zhou L, Liu W. Effect of Galangal Essential Oil Emulsion on Quality Attributes of Cloudy Pineapple Juice. Frontiers in Nutrition. 2021; 8: 751405.
[53] Zaidi SF, Muhammad JS, Shahryar S, Usmanghani K, Gilani AH, Jafri W, *et al*. Anti-inflammatory and cytoprotective effects of selected Pakistani medicinal plants in Helicobacter pylori-infected gastric epithelial cells. Journal of Ethnopharmacology. 2012; 141: 403–410.
[54] Zhao Y, Zhao K, Jiang K, Tao S, Li Y, Chen W, *et al*. A Review of Flavonoids from Cassia Species and their Biological Activity. Current Pharmaceutical Biotechnology. 2016; 17: 1134–1146.
[55] Batiha GES, Beshbishy AM, Ikram M, Mulla ZS, El-Hack MEA, Taha AE, *et al*. The Pharmacological Activity, Biochemical Properties, and Pharmacokinetics of the Major Natural Polyphenolic Flavonoid: Quercetin. Foods. 2020; 9: 374.
[56] Kim JH, Kang DM, Cho YJ, Hyun JW, Ahn MJ. Medicarpin Increases Antioxidant Genes by Inducing NRF2 Transcriptional Level in HeLa Cells. Antioxidants. 2022; 11: 421.

[57] Xu L, Li Z, Guo F. Curcumin improves expression of ghrelin through attenuating oxidative stress in gastric tissues of streptozotocin-induced diabetic gastroparesis rats. European Journal of Pharmacology. 2013; 718: 219–225.
[58] Phillips LK, Deane AM, Jones KL, Rayner CK, Horowitz M. Gastric emptying and glycaemia in health and diabetes mellitus. Nature Reviews. Endocrinology. 2015; 11: 112–128.
[59] Vieira-Frez FC, Sehaber-Sierakowski CC, Perles JVCM, Bossolani GDP, Verri WA, Jr, Nascimento RCD, *et al*. Anti- and pro-oxidant effects of quercetin stabilized by microencapsulation on interstitial cells of Cajal, nitrergic neurons and M2-like macrophages in the jejunum of diabetic rats. Neurotoxicology. 2020; 77: 193–204.
[60] Abdou HM, Abd Elkader HTAE. The potential therapeutic effects of Trifolium alexandrinum extract, hesperetin and quercetin against diabetic nephropathy via attenuation of oxidative stress, inflammation, GSK-3β and apoptosis in male rats. Chemico-biological Interactions. 2022; 352: 109781.
[61] Tang L, Li K, Zhang Y, Li H, Li A, Xu Y, *et al*. Quercetin liposomes ameliorate streptozotocin-induced diabetic nephropathy in diabetic rats. Scientific Reports. 2020; 10: 2440.
[62] Alkhalidy H, Moore W, Wang Y, Luo J, McMillan RP, Zhen W, *et al*. The Flavonoid Kaempferol Ameliorates Streptozotocin-Induced Diabetes by Suppressing Hepatic Glucose Production. Molecules. 2018; 23: 2338.
[63] Alshehri AS, El-Kott AF, Eleawa SM, El-Gerbed MSA, Khalifa HS, El-Kenawy AE, *et al*. Kaempferol protects against streptozotocin-induced diabetic cardiomyopathy in rats by a hypoglycemic effect and upregulating SIRT1. Journal of Physiology and Pharmacology. 2021; 72: 339–355.
[64] Alkhalidy H, Moore W, Wang A, Luo J, McMillan RP, Wang Y, *et al*. Kaempferol ameliorates hyperglycemia through suppressing hepatic gluconeogenesis and enhancing hepatic insulin sensitivity in diet-induced obese mice. The Journal of Nutritional Biochemistry. 2018; 58: 90–101.
[65] Sharma D, Kumar Tekade R, Kalia K. Kaempferol in ameliorating diabetes-induced fibrosis and renal damage: An in vitro and in vivo study in diabetic nephropathy mice model. Phytomedicine. 2020; 76: 153235.
[66] Alshehri AS. Kaempferol attenuates diabetic nephropathy in streptozotocin-induced diabetic rats by a hypoglycaemic effect and concomitant activation of the Nrf-2/Ho-1/antioxidants axis. Archives of Physiology and Biochemistry. 2021; 1–14.
[67] Wang Y, Yang R, Yan F, Jin Y, Liu X, Wang T. Medicarpin Protects Cerebral Microvascular Endothelial Cells Against Oxygen-Glucose Deprivation/Reoxygenation-Induced Injury via the PI3K/Akt/FoxO Pathway: A Study of Network Pharmacology Analysis and Experimental Validation. Neurochemical Research. 2022; 47: 347–357.
[68] Jin Y, Yang P, Wang L, Gao Z, Lv J, Cui Z, *et al*. Galangin as a direct inhibitor of vWbp protects mice from Staphylococcus aureus-induced pneumonia. Journal of Cellular and Molecular Medicine. 2022; 26: 828–839.
[69] Liu Y, Liang X, Zhang G, Kong L, Peng W, Zhang H. Galangin and Pinocembrin from Propolis Ameliorate Insulin Resistance in HepG2 Cells via Regulating Akt/mTOR Signaling. Evidence-based Complementary and Alternative Medicine. 2018; 2018: 7971842.
[70] Aladaileh SH, Al-Swailmi FK, Abukhalil MH, Shalayel MH. Galangin protects against oxidative damage and attenuates inflammation and apoptosis via modulation of NF-κB p65 and caspase-3 signaling molecules in a rat model of diabetic nephropathy. Journal of Physiology and Pharmacology. 2021; 72: 35–44.
[71] Wang J, Zhang L, Zhu J, Gu J, Wang X, Tao H. Hyaluronic Acid Modified Curcumin-Loaded Chitosan Nanoparticles Inhibit Chondrocyte Apoptosis to Attenuate Osteoarthritis via Up-regulation of Activator Protein 1 and RUNX Family Transcription Factor 2. Journal of Biomedical Nanotechnology. 2022; 18: 144–157.
[72] Zhang X, Zhang Y, Zhou M, Xie Y, Dong X, Bai F, *et al*. DPHC From *Alpinia officinarum* Ameliorates Oxidative Stress and Insulin Resistance *via* Activation of Nrf2/ARE Pathway in db/db Mice and High Glucose-Treated HepG2 Cells. Frontiers in Pharmacology. 2022; 12: 792977.
[73] Huang X, Liu G, Guo J, Su Z. The PI3K/AKT pathway in obesity and type 2 diabetes. International Journal of Biological Sciences. 2018; 14: 1483–1496.
[74] Zhang CM, Huang X, Lu HL, Meng XM, Liu DH, Kim YC, *et al*. Up-regulation of the Ang II/AT1 receptor may compensate for the loss of gastric antrum ICC via the PI3k/Akt signaling pathway in STZ-induced diabetic mice. Molecular and Cellular Endocrinology. 2016; 423: 77–86.